Endothelial inflammation: the role of differential expression of N-deacetylase/N-sulphotransferase enzymes in alteration of the immunological properties of heparan sulphate

Noel M. Carter[2], Simi Ali[1] and John A. Kirby[1,*]

[1]Applied Immunobiology Research Group, Department of Surgery, University of Newcastle, The Medical School, Newcastle upon Tyne NE2 4HH, UK
[2]Institute of Pharmacy, Chemistry and Biomedical Science, University of Sunderland, Sunderland SR1 3SD, UK
*Author for correspondence (e-mail: j.a.kirby@ncl.ac.uk)

Accepted 12 May 2003
Journal of Cell Science 116, 3591-3600 © 2003 The Company of Biologists Ltd
doi:10.1242/jcs.00662

Summary

Heparan sulphate N-deacetylase/N-sulphotransferase (NDST) enzymes catalyse the reaction that initiates sulphation and subsequent modification of the oligosaccharide, heparan sulphate (HS). The extent and distribution of sulphate substitution on HS plays a vital role in regulation of the binding of a range of proteins, including IFN-γ, several interleukins and most chemokines. In this study, the expression of NDST transcripts was found to be non-uniform between a range of cell types, suggesting that different cells produce characteristic HS species. It was found that stimulation of the HMEC-1 microvascular endothelial cell line with the pro-inflammatory cytokines IFN-γ and TNF-α caused a transient decrease in the level of NDST-1 and -2 transcripts after 4 hours ($P<0.05$ and $P<0.01$ respectively), but the expression of NDST-1 increased above control levels after 16 hours ($P<0.01$). The change in NDST expression was concurrent with an increase in the abundance of sulphated HS epitopes on the cell surface; this was not caused by variation in the expression of proteoglycans or by changes in the rate of GAG turnover. Cytokine-stimulated endothelial cells also showed an increase in their potential to bind RANTES (CCL5); this was abrogated by chlorate blockade of sulphotransferase activity or by heparitinase cleavage of cell surface HS. Monolayers of cytokine-stimulated HMEC-1 also supported an enhanced leukocyte chemotactic response towards RANTES. This study demonstrated that pro-inflammatory cytokines can increase NDST expression leading to increased sulphation of HS and a corresponding increase in sequestration of functional RANTES at the apical surface of endothelial cells. This may enhance leukocyte extravasation at sites of inflammation.

Key words: Heparan sulphate, Inflammation, Chemokine, IFN-γ, TNF-α, RANTES

Introduction

The extracellular matrix (ECM) surrounding human cells is a complex structure containing carbohydrates and proteins, including the proteoglycans. The proteoglycans are a diverse family consisting of a core protein, which can be membrane associated, linked to one or more oligosaccharide members of the glycosaminoglycan (GAG) family. Heparan sulphate (HS), one of the most abundant GAGs, is synthesised as a repeated disaccharide of glucosamine and glucuronic acid, which is modified by a variable series of reactions including sulphation. It has been hypothesised that the specific pattern of sulphate residues on mature HS plays a role in the regulation of diverse cellular functions, including development and immunity (Perrimon and Bernfield, 2000).

Previous work has shown that a number of important pro-inflammatory cytokines, including IFN-γ, some interleukins and most chemokines (Lortat-Jacob et al., 1995; Morita et al., 1994; Proudfoot et al., 2001; Rot et al., 1996) interact specifically with HS. This interaction is often focused at specific sequence domains within the HS oligomer which are characterised by extensive N-sulphation. Generation of these sequence domains is regulated during HS biosynthesis in the Golgi apparatus (Gallagher, 1997). The HS copolymer is attached to a core protein via a tetrasaccharide linkage and extended by alternate transfer from UDP-sugar donors of N-acetyl-D-glucosamine and D-glucuronic acid monomers. As the chain extends, it is potentially modified by the addition of sulphate residues at the amino group of glucosamine (N-sulphation) and at a range of hydroxyl groups (O-sulphation) within the disaccharide unit. Additionally, glucuronic acid may be modified by epimerisation of carbon 5 (C-5) to form iduronic acid. The O-sulphation and epimerisation modifications are dependent on the initial replacement of the N-acetyl group of glucosamine with an N-sulphate group (Unger et al., 1991); for example, the C-5 epimerase activity requires N-sulphation of an adjacent glucosamine (Li et al., 1997). The family of enzymes responsible for this important regulatory reaction are the N-deacetylase/N-sulphotranferases (NDSTs), of which there are four known human homologues (NDST-1, -2, -3 and -4). Whilst these enzymes share the same

basic function they do appear to have subtly different activities, with NDST-3 and -4 being expressed at low levels and with a restricted distribution (Aikawa et al., 2001).

The interaction between certain cytokines and sulphated domains on HS are ionic in nature, forming between basic amino acid sequences on the protein and anionic, sulphated domains on the GAGs (Lortat-Jacob et al., 1995; Morita et al., 1994; Pye et al., 1998). This interaction has a number of important functions, including protection, concentration and presentation of cytokines which are produced in small quantities by a small number of cells within the microenvironment. This process is believed to be of particular importance for presentation of chemokines on the surface of endothelial cells (Tanaka et al., 1996) and for stabilisation of the concentration gradients necessary for leukocyte chemotaxis (Adams and Lloyd, 1997; Ali et al., 2002; Appay and Rowland-Jones, 2001; Patel et al., 2001; Witt and Lander, 1994).

Heparin is structurally similar to HS, but is more uniformly sulphated along the GAG chain making it the most negatively charged molecule in the body. In many cases the amino acid sequences required for protein interaction with heparin have been defined as XBBXBX or XBBBXXBX, where B represents a basic residue (Hileman et al., 1998). The heparin binding properties of many chemokines, including the prototypical CC-chemokine RANTES (CCL5), which contain the XBBXBX motif within their primary sequence have been extensively studied (Kuschert et al., 1999). It has been shown that RANTES shows selectivity with regards to GAG binding, with its affinity for heparin being three orders of magnitude greater than for chondroitin sulphate; site-directed mutation has shown that the XBBXBX motif on RANTES is a principal site for heparin binding (Kuschert et al., 1999; Proudfoot et al., 2001).

Previous work has shown marked differences in the expression of NDST transcripts between both tissues and different species (Aikawa et al., 2001; Habuchi et al., 2000; Shworak et al., 1999). However, few studies have compared the levels of NDST expression between individual cell types or studied how expression of these molecules is modulated by external stimuli. Given the important function of chemokine binding to endothelial HS during inflammation and the dependence of this process on the extent of sulphation of the GAG molecule, this study was designed to investigate the role of modulation of HS sulphation during endothelial inflammation. Northern blotting and RT-PCR analysis were used to study the expression of individual NDST transcripts and a range of functional assays were used to investigate how changes in NDST expression correlated with sequestration of RANTES by endothelial cells.

Materials and Methods

Cell lines and media

The HMEC-1 microvascular endothelial cell line (Ades et al., 1992) (kindly provided by Dr F. J. Candal, CDC, Atlanta, USA) was grown in MCDB-131 medium (Sigma) containing 1 ng/ml hydrocortisone (Sigma) and 10 ng/ml human epidermal growth factor (Peprotech). A549 (ECACC 86012804; ECACC) and U937 (ECACC 85011440; ECACC) cells were grown in RPMI-1640 (Gibco). The cell lines Hep-G2 (ECACC 85011430; ECACC) and HEK 293 (ECACC 85120602; ECACC) were grown in Dulbecco's modified Eagle's medium (Gibco). The HMC-1 cell line (Butterfield et al., 1988) was grown in Iscove's modified Dulbecco's medium (Gibco), supplemented with 5×10^{-5} M 2-mercaptoethanol. All media were additionally supplemented with 10% fetal bovine serum (Sigma) and penicillin-streptomycin (Gibco).

RNA extraction and purification

Cell lines were grown to confluency and total RNA extracted using RNAzol B reagent (AMS Biotech). Adherent cell lines (HMEC-1, A549, Hep G2 and HEK 293) were grown in 75 cm^2 flasks and were lysed in situ with 3 ml RNAzol reagent preheated to 70°C. Some HMEC-1 cultures were stimulated with 100 U/ml of both TNF-α and IFN-γ for 4 or 16 hours before the extraction of RNA. Suspension cell lines (HMC-1 and U937) were grown to confluency in 15 ml of media, pelleted and lysed with 3 ml RNAzol B reagent preheated to 70°C. Oligotex mRNA mini kits (Qiagen) were then used to purify the mRNA from the total RNA extracted using the RNAzol B reagent. RNA was quantified by measurement of absorbance at 260 nm and was stored at –20°C.

Northern blotting

RNA samples were electrophoresed in formaldehyde denaturing agarose gels and blotted onto Hybond XL nitrocellulose (Amersham Pharmacia). The amount of RNA loaded onto the gels was either 100 μg of total RNA or 1 μg of mRNA. The NDST-1 probe was prepared by random prime synthesis with 20 ng of PCR product as template and [α-^{32}P]dCTP (Amersham Pharmacia) for labelling. An antisense RNA probe for NDST-2 was prepared by transcription with T3 RNA polymerase from 1 μg of a linearised NDST-2 pBluescript II KS- clone; this probe was labelled with [α-^{32}P]UTP (Amersham Pharmacia). Excess nucleotides were removed from the probes by purification using Sephadex G-50 columns (Amersham Pharmacia).

Reverse transcription coupled PCR

First strand cDNA was synthesised using 0.5 μg of mRNA. Fragments of NDST-1 and -2 were initially amplified from cDNA using the proof reading polymerase *pfu* (Stratagene) for subsequent sequence verification. The exon-spanning primer sequences are shown below:

NDST1-forward (5′-CACACAGAACGAACTACGC-3′)
NDST1-reverse (5′-CCCGTTGATGATCTTGTCC-3′)
NDST2-forward (5′-GCCTCCAGTTCCACCTC-3′)
NDST2-reverse (5′-CGACGAAGAACTGGTCC-3′)

Amplifications were performed in a DNA thermal cycler (Hybaid) for 35 cycles under the following conditions: 94°C for 30 seconds, 58°C for 30 seconds and 72°C for 30 seconds. For the semi-quantitative analysis of expression, the amplification was dropped to 27 cycles and housekeeping transcripts of glyceraldehyde 3-phosphate dehydrogenase (Gap-DH) were analysed for comparison.

Antibodies and flow cytometric analysis

An anti-HS monoclonal antibody (F58-10E4; Seikagaku Corp) was used for primary cell surface labelling followed by secondary labelling with a FITC-conjugated goat anti-mouse polyclonal antibody (GAM-FITC; Becton Dickinson) before flow cytometric analysis. Expression of the promiscuous Duffy antigen receptor for chemokines (DARC; CD234) was also measured by immunofluorescence.

HMEC-1 cells were grown to confluence in 75 cm^2 flasks and stimulated with 100 U/ml of both TNF-α and IFN-γ in MCDB-131 medium; control cells were unstimulated. The cells were stimulated for periods between 16 and 72 hours prior to harvesting by incubation at 37°C for 10 minutes with 5 ml PBS containing 3 mM EDTA; in

some cases cytokine-stimulation was performed for 24 hours in the presence of cycloheximide at 10 μg/ml (Sigma). The cells released from a single culture flask were split into four aliquots. Primary antibody was added to three of these at a final concentration of 5 μg/ml, with the fourth being used for an isotype-matched (IgM) primary and secondary antibody control. The tubes were incubated at 4°C for 1 hour, washed again with PBS, resuspended in 50 μl of 10 μg/ml secondary antibody in PBS and incubated for 30 minutes at 4°C. The cells were then washed again and analysed by flow cytometry (FACsort; Becton Dickinson); the signal from control immunofluorescence did not change from autofluorescence levels. Data analysis was performed using FCS Express (De Novo software) and Excel (Microsoft).

GAG labelling and purification

GAGs were purified by incubating HMEC-1 cells for 24 hours with 2.5 μCi [^{3}H]glucosamine (Amersham). Cells were washed in PBS then stimulated with cytokines as above for 0, 4 or 16 hours. Cells were incubated for 1 hour in 0.1 N NaOH at 37°C after which they were neutralised with sodium acetate. The cell extracts were loaded onto a DEAE Sepharose column, washed with 0.3 M NaCl to remove contaminating proteins, and then eluted in 1.5 M NaCl (Esko, 2002). The relative amount of GAG present in each sample was estimated and the incorporated tritium measured by scintillation counting.

Western blotting to detect HS proteoglycans

This study was performed using methodology described previously (Olofsson et al., 1999). Briefly, cells were detached from confluent 75 cm^2 flasks by washing with PBS containing 3 mM EDTA and then incubation for 10 minutes at 37°C in 5 ml of the same solution. The cells were then washed by centrifugation in PBS and resuspended in a solution containing 10 mU/ml heparatinase (Seikagaku Corp), 0.5 U/ml chondroitinase ABC (Seikagaku Corp), 100 mM NaCl, 1 mM $CaCl_2$, 0.1% Triton X-100, 50 nM 6-aminohexanoic acid, 20 μg/ml leupeptin, 2.5 μg/ml pepstatin A, 1 mM PMSF, and 50 mM Hepes at pH 7.0 before incubation at 37°C for 3 hours. The samples were run under non-reducing conditions by SDS-PAGE and transferred to hybond-P membranes (Amersham Pharmacia). In order to get good separation of all proteins, the samples were run on both 12% and 8% acrylamide gels. Immunoblotting was performed with mouse antibody 3G10 (Seikagaku Corp.) followed by goat anti-mouse immunoglobulin conjugated to horseradish peroxidase (Pharmingen). The 3G10 antibody is specific for a neo-epitope generated on HS 'stubs' which remain attached to proteoglycan core proteins after heparitinase digestion (David et al., 1992). Bound antibody was detected using the ECL substrate (Amersham Pharmacia). Following primary development the blots were stripped and re-probed with a mouse antibody specific for α-tubulin (Sigma) to control for equal protein loading.

Measurement of RANTES binding

The HMEC-1 cell line was grown to confluency in MCDB-131 medium in chamber slides (Falcon). The cells were stimulated for 16 hours with fresh media containing 100 U/ml IFN-γ and 100 U/ml TNF-α either with or without 100 mM sodium chlorate; none of these treatments was toxic during this period. Chlorate is a reversible inhibitor of the enzyme ATP sulphurylase, which produces the 3′-phosphoadenosine-5′-phosphosulphate substrate required for sulphotransferase activity (Safaiyan et al., 1999). Further cells were treated with 10 mU of heparitinase (Seikagaku Corp) for 3 hours at 37°C to deplete cell surface HS. Control cells were grown in medium alone. After incubation, the cells were fixed in cold methanol and the chamber well was removed from the slide. The cells were rehydrated with PBS and were covered with 150 μl PBS containing 200 ng of RANTES (Peprotech) for 16 hours. After washing, the cells were incubated with 10 μg/ml of mouse anti-RANTES (Caltag) for 3 hours at 4°C before incubation for 1.5 hours with 10 μg/ml GAM-FITC (Becton Dickenson). The slides were washed and mounted using Vectorshield (Vectorlabs) before analysis by scanning laser confocal microscopy using Comos v7 software (Biorad). Control preparations were routinely incubated with and without RANTES to distinguish between exogenous and endogenously produced chemokine; an isotype-matched primary control antibody (IgG2b) produced no significant immunofluorescence.

Radioligand binding experiments

The binding of ^{125}I RANTES to HMEC-1 cells was assessed in 12 well plates. Each well was seeded with 1×10^4 cells, which were grown to confluency. The cells were then washed and treated with either 100 U/ml of both TNF-α and IFN-γ, 100 U/ml of TNF-α and IFN-γ in 100 mM sodium chlorate, or medium only. The cells were all left for a further 4 or 16 hours before fixation in cold methanol for 10 minutes, washing with PBS and incubation for 2 hours at 37°C in PBS containing 377 pM ^{125}I-RANTES and 300 nM of unlabelled RANTES. The cells were washed twice with PBS to remove any unbound ligand. The cells were then lysed by incubation at 37°C for 1 hour in a solution of 0.1 M NaOH and transferred to test tubes; the radioactivity was then measured by gamma counting (Clinigamma, Wallac UK).

Chemotaxis assay

HMEC-1 monolayers were propagated on 24-well format transwell membranes (3 μm pore; Falcon plastic) by seeding each with 4×10^5 cells in supplemented MCDB-1 medium and culturing for 72 hours; some monolayers were activated with TNF-α and IFN-γ for 100 U/ml for the final 24 hours. The monocyte cell line THP-1 (ATCC TIB 202) was cultured in RPMI1640 medium supplemented in 10% foetal calf serum and activated with 100 U/ml IFN-γ for 24 hours to enhance their chemotactic response (data not shown). For chemotaxis assays the lower compartment of each transwell chamber was filled either with normal medium or medium supplemented with RANTES at 10 ng/ml and the chambers were cultured for 30 minutes to allow chemokine distribution within the monolayer. One million THP-1 cells were then added to the upper compartment of each chamber and the system was incubated for 90 minutes. After this time the upper surface of each membrane was wiped clear of excess cells and the membranes were fixed in methanol at –20°C before staining with Haematoxylin and mounting; the mean number of migrant cells per high power field was determined by microscopic examination of the lower surface of each filter.

Statistical analysis

All groups were compared with the corresponding control using Student's two-sample *t*-test. All groups were measured as triplicates and P values <0.05 were considered significant.

Results

Expression of NDST transcripts

NDST-1 and -2 could be amplified by PCR from the cDNA libraries produced from each of the cultured cell lines (data not shown). However, published primer sequences failed to amplify either NDST-3 or -4 transcripts from any of the cell lines (Aikawa et al., 2001). PCR fragments generated for NDST-1 and -2 were cloned into pBluescript II KS– and verified by DNA sequence analysis; all clones showed 100% homology with the published sequences.

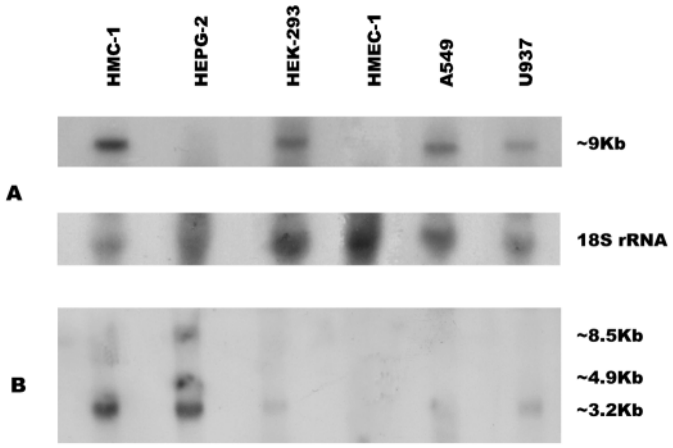

Fig. 1. Expression of NDST-1 and -2 transcripts by different cell types. Samples were run in a 1.5% agarose gel; for each sample 100 μg of total RNA (A), or 1 μg of poly(A)$^+$ RNA (B) was run and blotted onto a nylon membrane. RNA was isolated from the cell types displayed at the top of the figure. Northern blot analysis was performed using a random prime synthesised probe using [^{32}P]dCTP for NDST-1 (A) and an antisense probe labelled with [^{32}P]UTP for NDST-2 (B). The bands showing 18S rRNA within the total RNA indicate the relative loading of each of the samples. The size of the RNA species was determined by co-electrophoresis of mRNA size standards (Promega).

Fig. 1 shows the northern blots for NDST-1 and -2 (Fig. 1A and B, respectively); the data and nature of the cells is summarised in Table 1. The pattern of gene expression differed between all the cell types except the two epithelial cell lines (HEK-293 and A549), which showed broadly similar transcript expression. Neither NDST-1 nor NDST-2 could be detected in the resting HMEC-1 cell line by northern blotting.

Semi-quantitative RT-PCR analysis of the HMEC-1 cell line

The low detectable levels of NDST expression in the HMEC-1 cell line led to further investigation by semi-quantitative RT-PCR. It is possible that levels of expression may be tightly regulated in order to respond more efficiently to external stimuli. In order to test this hypothesis the HMEC-1 cell line was stimulated with the pro-inflammatory cytokines TNF-α and IFN-γ. The level of expression of NDST-1 and -2 was then examined by semi-quantitative RT-PCR. Expression of the chemokine RANTES was used as a positive control as this transcript is known to be upregulated under these conditions (Mantovani et al., 1997). Fig. 2 shows the level of expression of NDST-1, -2 and RANTES following stimulation with the pro-inflammatory cytokines TNF-α and IFN-γ for 4 or 16 hours (Fig. 2A and B, respectively). By 4 hours post-stimulation there was a significant downregulation of both NDST-1 (P<0.05) and NDST-2 expression (P<0.01), with upregulation of the chemokine RANTES (P<0.001) providing a positive control. After 16 hours the situation was reversed with NDST-1 now showing significant upregulation (P<0.01) and NDST-2 also showing an increase, although this did not reach significance (P<0.08). Once again, RANTES expression was significantly higher than the control (P<0.005).

Table 1. Summary of northern blot data from Fig. 1

Cell line	NDST 1 expression	NDST 2 expression	Cell type
HMC-1	+++	+++	Mast
HepG-2	–	+++	Hepatocyte
HEK-293	+++	+/–	Epithelial (kidney)
HMEC-1	–	–	Endothelial
A549	+++	+/–	Epithelial (lung)
U937	++	+	Monocyte

The level of expression is indicated as follows: high, +++; medium, ++; low, +; very low, +/–; no expression, –.

Analysis of HMEC-1 phenotype

The monoclonal antibody 10E4 was used to define the abundance of sulphated domains within HS on the endothelial cell surface. The specificity of this antibody was demonstrated by David et al., (David et al., 1992) who showed that binding to HS was completely abrogated by selective desulphation to produce an N-desulphated HS molecule which retained O-sulphated groups. Antibody

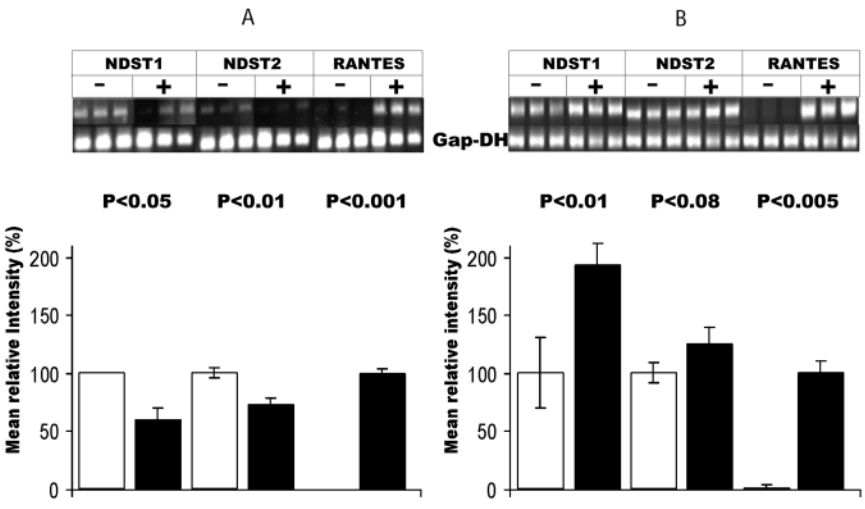

Fig. 2. Semi-quantitative analysis of NDST-1 and -2 transcript expression by the HMEC-1 cell line. Semi-quantitative RT-PCR analysis was carried out for HMEC-1 cells both 4 hours (A) and 16 hours (B) after stimulation with the pro-inflammatory cytokines TNF-α and IFN-γ; the results were compared with data from resting cells. The RANTES transcript was also examined as a positive control and Gap-DH was examined as an internal standard. The gel images show the RT-PCR products generated from unstimulated (–) or stimulated (+) HMEC-1 cells with their respective Gap-DH products. The white bars in the graphs show the mean relative band intensity for the unstimulated control cells and are normalised to 100%. The black bars represent the mean relative band intensity for the cells stimulated with TNF-α and IFN-γ. The P values above the bars show the significance of differences between the data sets.

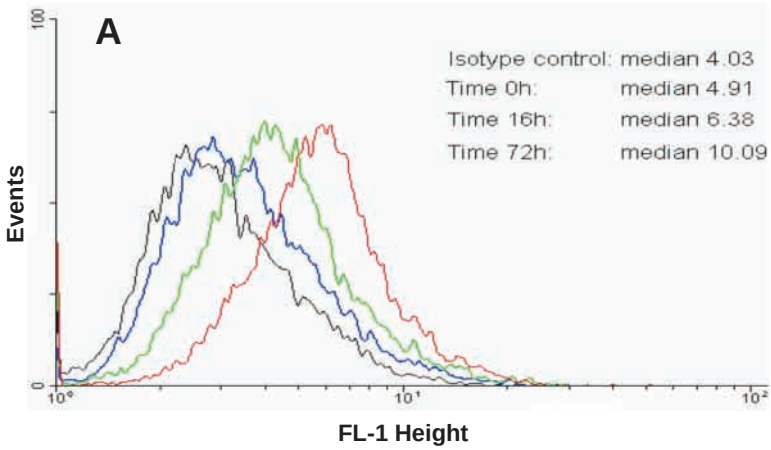

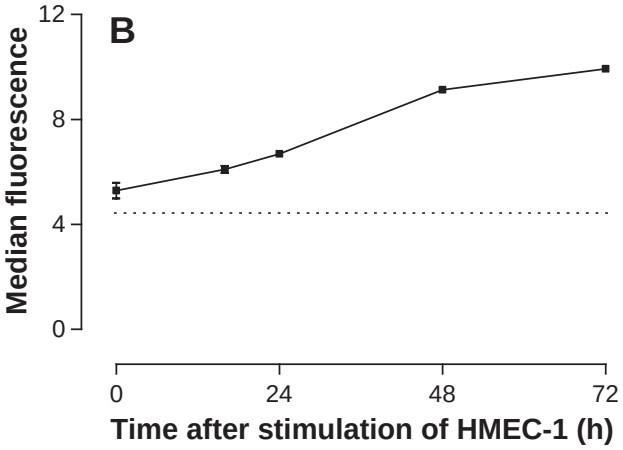

Fig. 3. Phenotypic analysis of the abundance of sulphated epitopes in HS. HMEC-1 cells were analysed by flow cytometry to measure the level of sulphation at 0, 16, 24, 48 and 72 hours after stimulation with TNF-α and IFN-γ. (A) Representative flow cytometer fluorescence histograms showing the isotype control value (black) and data from time 0 (blue), 16 (green) and 72 hours (red); median values are also shown. (B) Summary results showing the increase in fluorescence due to binding of 10E4 antibodies to cytokine activated HMEC-1 cells; the dotted line indicates the upper level of isotype control fluorescence. Data points show the mean from triplicate determinations; the error bars indicate the s.e.m.

binding was restored following re-N-sulphation of the molecule, but no binding was observed after re-N-acetylation. HMEC-1 cells were analysed by FACS to observe the levels of cell surface HS sulphation on resting cells and after stimulation for 16, 24, 48 and 72 hours with the cytokines TNF-α and IFN-γ. Fig. 3A shows representative flow cytometric histograms which demonstrate an increase in binding of the 10E4 antibody, and hence in expression of N-sulphated epitopes, with time following cytokine stimulation of the cells. Importantly, no increase in the binding of 10E4 antibodies to cytokine-stimulated cells was observed in the presence of cycloheximide, indicating a requirement for protein synthesis (data not shown). The summary data in Fig. 3B indicate little 10E4 antibody binding above isotype control levels at time 0 but an increase in median fluorescence was observed after cytokine-stimulation for 16 hours and it continued to increase for 72 hours ($P<0.005$). The cells expressed very low levels of cell surface DARC; this was not increased following cytokine stimulation of the cells (data not shown).

Analysis of cell surface GAG turnover by cytokine-stimulated HMEC-1 cells

A pulse-chase experiment was performed to measure the rate of GAG turnover in order to detect any effect of treatment of HMEC-1 cells with pro-inflammatory cytokines. HMEC-1 cells were cultured overnight with [^{3}H]glucosamine. The cells were then washed, returned to unlabelled media and allowed to grow for a further 4 or 16 hours under normal conditions or in the presence of TNF-α and IFN-γ. The GAG complement of the cells was then purified and the amount of incorporated tritium was measured. Fig. 4 shows that the amount of radiolabelled glucosamine falls over time, indicating GAG turnover. However, after 4 and 16 hours the level of incorporation was the same for both unstimulated and cytokine-stimulated cells ($P>0.05$), suggesting that the rate of turnover remained the same under both conditions. This suggests that changes in cell surface sulphation occur as a consequence of modification of newly synthesised HS; there appears to be no enhanced shedding of GAGs by the cytokine stimulated cells.

Quantification of HS proteoglycans by western blotting

Increases in the abundance of sulphated HS epitopes on the

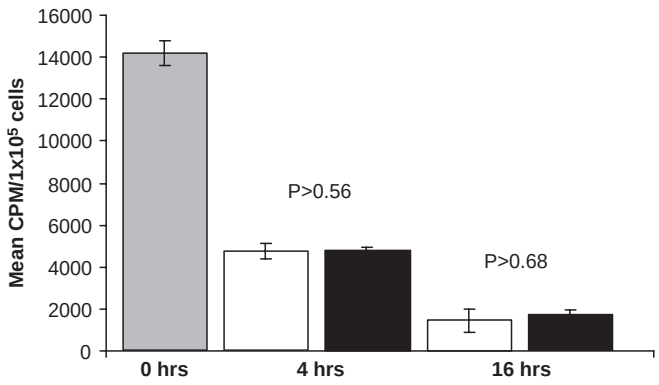

Fig. 4. Analysis of the kinetics of GAG turnover. HMEC-1 cells were labelled with ^{3}H-glucosamine for 24 hours and were then washed and cultured either with or without TNF-α and IFN-γ. The cells were harvested after 4 hours and 16 hours, the GAGs were purified and incorporated ^{3}H was measured. Bars represent the mean relative cpm for GAG derived from 10^5 cells. The sample at 0 hours (shaded) provides a measure of the initial level of incorporation. The white bars represent unstimulated cells and the black bars indicate cells stimulated with TNF-α and IFN-γ. The *P* values above the bars indicate the significance of differences between the unstimulated and stimulated groups after 4 hours and 16 hours; the error bars show the s.e.m.

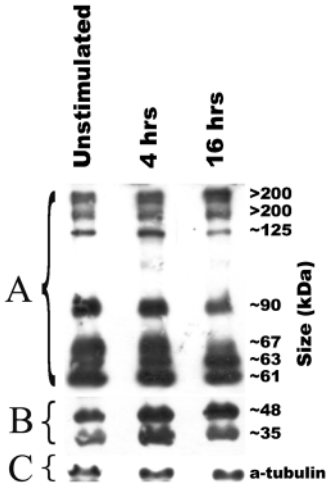

Fig. 5. Analysis of proteoglycan core protein expression by western blotting. Lysates from HMEC-1 cells stimulated for 4 hours or 16 hours with TNF-α and IFN-γ were compared with those from unstimulated cells. All lysates were digested in the presence of chondroitinase ABC and heparatinase. The cleavage products were separated by SDS-PAGE, electrotransferred to hybond-P membranes and probed by mAb 3G10. The figure is a composite generated from gels containing 8% (A) and 12% (B) acrylamide, as indicated. Blots were reprobed with an anti α(a)-tubulin antibody to provide an internal protein loading control (C). Apparent molecular masses of the core proteins are indicated.

surface of cytokine-stimulated HMEC-1 could occur as a consequence of increased synthesis of HS proteoglycans. In order to investigate this, a series of quantitative western-blotting experiments was performed using the 3G10 antibody, which recognises residual unsaturated glucuronate stubs on all HS proteoglycan core proteins (David et al., 1992). Fig. 5 shows a composite of blots run on both 8 and 12 percent acrylamide gels. The HS stub-bearing core proteins are visible as multiple bands between 200 kDa and 35 kDa and appear to be predominantly a mixture of glypicans and syndecans. There was no increase in the density of these bands relative to the corresponding control α-tubulin band following stimulation with TNF-α and IFN-γ. Indeed, the bands at 90 kDa and 78 kDa showed a small reduction in intensity after 16 hours. The absence of an increase in the quantity of proteoglycan-associated HS stubs following cytokine stimulation of the HMEC-1 cells indicates that the increase observed in HS sulphation (10E4 antibody binding) occurs at the level of the individual GAG molecules.

Examination of the binding of exogenous RANTES to HMEC-1 cells

As RANTES is known to bind to sulphated domains on HS, a series of experiments was performed to determine whether treatment of endothelial cells with pro-inflammatory cytokines resulted in an increased potential for RANTES sequestration by HS molecules following upregulation of NDST-1 and -2. Fig. 6 shows the results from an immunofluorescence scanning laser confocal microscope study of the binding of exogenous RANTES to resting, cytokine-stimulated and resting HMEC-1. Little surface-

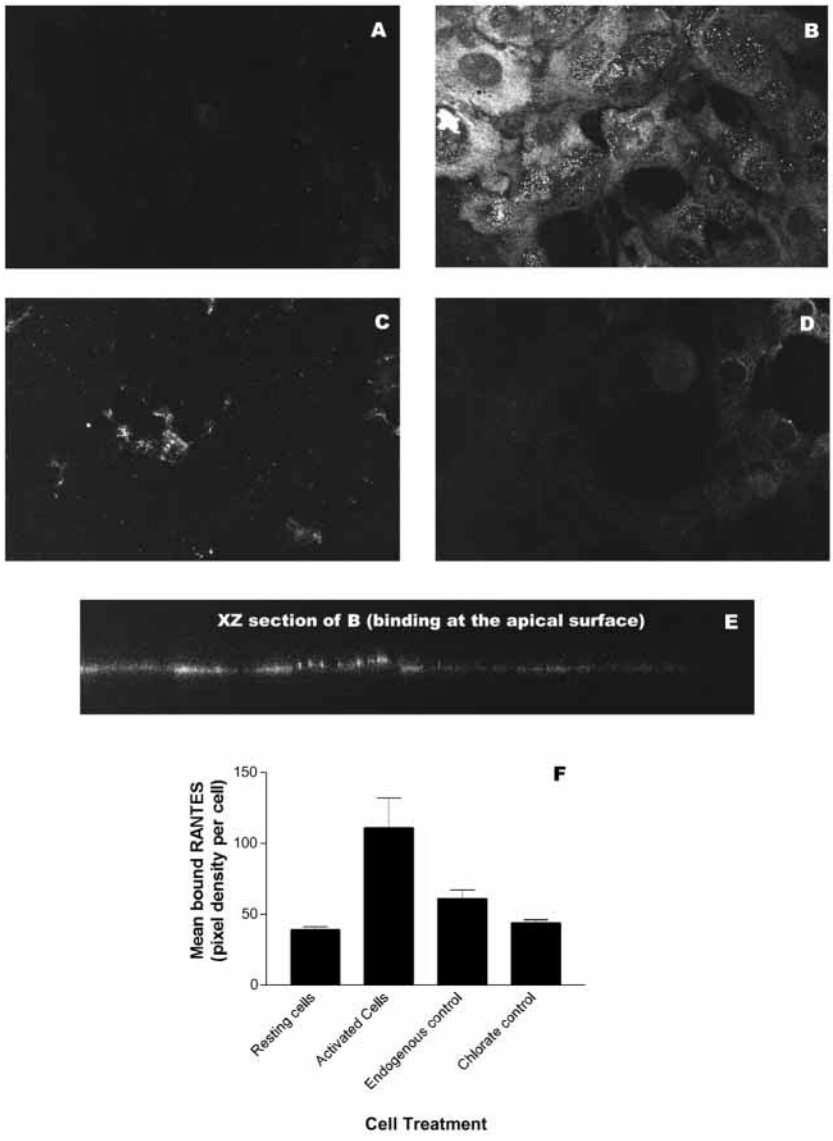

Fig. 6. Immunofluorescence detection of RANTES binding to HMEC-1 cells. Scanning laser confocal microscopy was used to analyse the distribution of RANTES on the surface of HMEC-1 cells that had been cultured using a range of experimental conditions. (A) RANTES expression on the surface of resting HMEC-1 which had been treated with exogenous RANTES. (B) RANTES expression on the surface of HMEC-1 that had been stimulated with TNF-α and IFN-γ and then treated with exogenous RANTES. (C) Expression of endogenous RANTES on the surface of HMEC-1 that had been stimulated with TNF-α and IFN-γ. (D) RANTES expression on the surface of HMEC-1 cells that had been stimulated with TNF-α and IFN-γ in the presence of chlorate and then treated with exogenous RANTES. (E) A constructed X-Z section through Fig. 6B confirming that binding of the exogenous RANTES occurs only on the apical surface of the cultured endothelial cells. (F) Summary data showing inverted mean fluorescence pixel intensity per cell for each of the four treatment groups; the resting and (cytokine) activated groups were treated with exogenous RANTES, the endogenous control group was cytokine-activated but received no exogenous RANTES and the chlorate control group was cytokine activated and received exogenous RANTES. The error bars show the s.e.m.

bound RANTES was observed following chemokine addition to unstimulated HMEC-1 (Fig. 6A). However, following stimulation with TNF-α and IFN-γ for 16 hours a greater amount of the added chemokine was bound to the cell surface (Fig. 6B); at this time, endogenously produced RANTES made a minimal contribution to cell-surface chemokine expression (Fig. 6C). Cells stimulated with TNF-α and IFN-γ in the presence of chlorate (an inhibitor of GAG sulphation) also bound minimal quantities of exogenous RANTES (Fig. 6D). Removal of HS from cytokine-stimulated cells by treatment with heparitinase also reduced subsequent RANTES binding to background levels (data not shown). Construction of a X-Z image through Fig. 6B (shown in Fig. 6E) shows that exogenous RANTES was bound on the apical surface of cytokine-stimulated HMEC-1. Mean results from semi-quantitative analysis of cell-associated fluorescence are shown in Fig. 6F; this graph shows a 2.8-fold increase in RANTES binding to cytokine-activated cells ($P<0.01$) which cannot be accounted for by the detection of RANTES produced endogenously by the activated cells. Furthermore, blockade of GAG sulphation reduced RANTES binding by cytokine-activated cells to levels associated with resting cells ($P>0.05$); this excluded the possibility that the increase in chemokine-binding was caused by upregulated expression of any known or unknown specific chemokine receptors.

Radioligand quantification of RANTES binding to HMEC-1 cells

A further series of experiments was performed to investigate the binding of RANTES to endothelial cells; ligand binding was performed at physiological salt concentrations to prevent disruption of ionic protein-GAG interactions. Fig. 7 shows that stimulation of the cells for 16 hours with TNF-α and IFN-γ produced a 40% increase in RANTES binding ($P<0.002$); this increase was not observed for cells stimulated with pro-inflammatory cytokines in the presence of chlorate. Again this shows that the binding of RANTES to HMEC-1 endothelial cells increases after stimulation with pro-inflammatory cytokines and suggests that this increase is dependent on GAG sulphation rather than binding to any specific receptor.

Transendothelial leukocyte chemotaxis

A series of experiments was performed to assess the potential of RANTES to induce vectorial migration of monocytes across monolayers of resting or cytokine-activated HMEC-1 cells. It was found that neither resting nor activated endothelium supported efficient leukocyte migration in the absence of exogenous RANTES applied to the basal surface of the monolayer. However, the addition of RANTES caused a significant increase in migration across both resting and cytokine-activated endothelial cell monolayers. Importantly, comparison of the chemotactic response across resting and cytokine-activated HMEC-1 showed that the activated monolayer supported the migration of 3.4-fold more leukocytes per unit area (Fig. 8; $P<0.0001$).

Discussion

This paper addresses the hypothesis that the expression of members of the NDST enzyme family can vary between

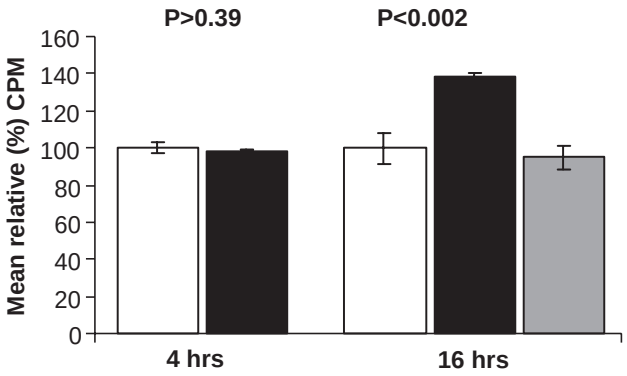

Fig. 7. Radioligand quantification of RANTES binding to HMEC-1 cells. HMEC-1 cells were grown in the presence of medium alone (white bars), TNF-α and IFN-γ (black bars) or TNF-α and IFN-γ in the presence of 100 mM sodium chlorate (shaded bar). The cells were then treated with ^{125}I-RANTES and the bound isotope was subsequently determined and expressed as counts per cell; data from the untreated control cells was normalised to 100% and the treated cells were measured relative to this value. The p value above the bars indicates the significance of differences between the unstimulated and stimulated groups after 4 hours and 16 hours; error bars show the s.e.m.

different cell types and following stimulation by pro-inflammatory cytokines. The immortalized human microvascular endothelial cell line HMEC-1 was used to model the effect of cytokine-mediated regulation of NDST expression on the abundance of sulphated domains within HS on the surface of the vascular endothelium. This was followed by an examination of changes in the potential of these cells to bind exogenous RANTES at their apical surface and subsequent analysis of changes in the biological activity of this chemokine. The HMEC-1 cell line was chosen for this work as it provides a reproducible system which has previously been validated to model aspects of the immunobiology of microvascular endothelium including the uniform response to pro-inflammatory cytokines (Goebeler et al., 1997) and the presentation of antigens to specific T cells (Bosse et al., 1993). In addition, HMEC-1 cells are already known to use cell surface HS to bind exogenous proteins (Robinson et al., 2002).

Northern analysis of members of the NDST family showed clearly, and for the first time, that the pattern of NDST expression varies between different cell types, with a panel of 6 resting cell lines showing marked differences in their relative expression of NDST-1 and -2. In this study the gels were loaded with 100 μg of total RNA or 1 μg of mRNA; these relatively large amounts of RNA were used in order to detect low levels of transcription. For the NDST-2 blot, mRNA was used in order to reduce background binding to ribosomal RNA, which masked the transcripts when large amounts of total RNA were used. Similar patterns of NDST-1 and -2 expression were observed for the lung and kidney epithelial cells, but it cannot be concluded that this observation extends to all epithelial cells. Despite the high level of RNA loading, neither NDST-1 nor -2 was observed in preparations from resting HMEC-1 endothelial cells. Significantly, RT-PCR failed to detect expression of NDST-3 and -4 in any cell line. This is consistent with a previous study which showed that the expression of these two genes is highly restricted (Aikawa et al., 2001).

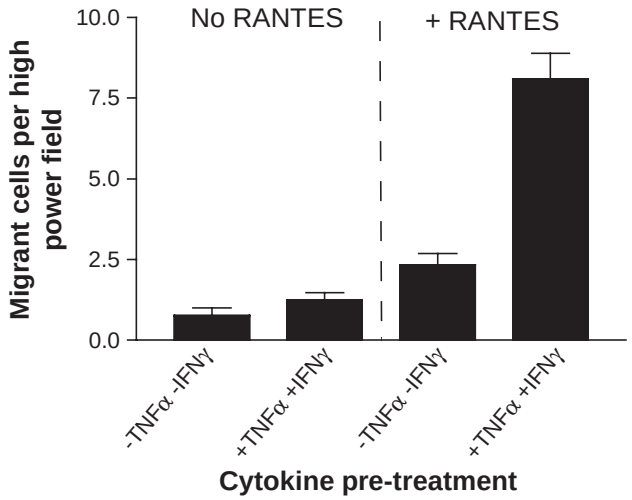

Fig. 8. Comparison of leukocyte chemotaxis across monolayers of resting and activated HMEC-1. The number of migrant THP-1 cells on the lower surface of each transwell filter was assessed by counting the cells per high power microscope field. The bars show the mean number of cells in 10 fields per filter; the error bars represent the s.e.m.

It is of interest that the transcript for NDST-1 was approximately 9 kb in length compared to a coding sequence of 2649 bp (Dixon et al., 1995); this suggests that the transcript contained extensive untranslated regions (UTRs). This is consistent with the large 3′-UTRs of up to ~5 kb observed during the sequencing of NDST-1 from a placental cDNA library (Dixon et al., 1995). The coding sequence for NDST-2 is 2652 bp (Humphries et al., 1998), but longer transcripts were again observed, indicating large UTRs. These UTRs may play a role in the regulation of message stability and expression. Indeed, a recent report by Grobe and Esko (Grobe and Esko, 2002) has highlighted a mechanism for post-transcriptional regulation of NDST expression in which the 3′-UTRs contain cryptic translation codons that might reduce the rate of translation. Three bands were observed on the NDST-2 blots, which is consistent with previous studies showing multiple NDST-2 transcripts (Kusche-Gullberg et al., 1998; Orellana et al., 1994; Toma et al., 1998). The observed high level expression of NDST-2 in the liver and mast cell lines is again consistent with results from a previous study (Orellana et al., 1994). The differing pattern of expression of mRNA encoding NDSTs between the cell lines is suggestive of variations in NDST function resulting in a change in the extent of N-sulphation within HS. This may result in differences in the potential of HS to bind extracellular proteins, leading to tissue-specific differences in protein function.

The failure of northern blotting to detect NDST expression in HMEC-1 endothelial cells suggests that the messages encoding these enzymes are normally expressed at a low level or are turned over rapidly, allowing detection only by RT-PCR. This observation is surprising, as it is known that HS constitutes up to 50% of the total GAG expressed by endothelial cells (Cockwell et al., 1996). However, the endothelium functions as the interface between blood and the tissues and must be able to respond dynamically to its microenvironment in order to regulate the passage of cells into sub-endothelial tissues during inflammatory immune responses (Rix et al., 1996). To achieve this it would be valuable for the endothelium to have a mechanism that enables rapid alteration of its potential to bind a wide range of pro-inflammatory factors in order to present them at the cell surface. Regulation (up or down) of the extent of HS sulphation within the cellular microenvironment would provide a candidate mechanism for increasing cytokine presentation during episodes of inflammation, and could allow the effect of these cytokines to be localised.

Analysis of the upstream sequence between bases –1 and –1000 of all four members of the NDST family (AliBaba 2.1; http://www.gene-regulation.com) was performed to detect potential transcription factor binding sites. Five putative Sp-1 binding sites were identified in the region –1 to –300 and another at position –970 of the NDST-1 sequence. Analysis of the NDST-2 sequence predicted five Sp-1 sites between –1 and –300, two between –400 and –500 and a further two between –800 and –900. These sites were not identified in the sequences of either NDST-3 or -4. The transcription factor Sp-1 is known to be induced by TNF-α and plays an important role in promoting the expression of vascular cell adhesion molecule-1 (VCAM-1) (Neish et al., 1995) and intercellular adhesion molecule-1 (ICAM-1) (Voraberger et al., 1991) by pro-inflammatory cytokine stimulated endothelial cells. This suggests a potential mechanism by which NDST-1 and -2 could be upregulated by pro-inflammatory cytokines.

Evidence presented in the current study implicates NDST upregulation as an important component of the activation of endothelial cells during episodes of inflammation. Stimulation of the endothelial cell line HMEC-1 with the pro-inflammatory cytokines TNF-α and IFN-γ produced significant changes in the level of expression of NDST-1 and -2, which correlated with changes in structure of HS on the cell surface. Interestingly, changes in the level of expression of NDST appeared to be bi-phasic following the stimulation of endothelial cells with pro-inflammatory cytokines. Initially the levels fell slightly, but significant increases in expression were observed after 16 hours; the expression of sulphated 10E4 epitopes on the cell surface was elevated after 16 hours and continued to increase for up to 72 hours. A previous study has shown that IFN-γ reduces the incorporation of sulphate into HS immediately after stimulation (Praillet et al., 1996c), whilst the presence of IFN-γ has been shown to increase the relative amount of HS compared to other GAGs, such as chondroitin sulphate (Praillet et al., 1996a; Praillet et al., 1996b). Differences between the binding of the 10E4 antibody to resting and cytokine-activated endothelial cells could not be explained by differential shedding of GAGs as no significantly enhanced loss of radioactivity was observed following stimulation of cells that had been pre-labelled with [^{3}H]glucosamine.

Flow cytometric data showed that pro-inflammatory cytokine-stimulation produced a change in the epitopic structure of HS at the endothelial cell surface which is likely to reflect an increase in the overall level of N- and, ultimately, O-sulphation. Previous studies have shown that overexpression of NDSTs can result in the production of HS with increased N- and O-sulphation (Cheung et al., 1996; Pikas et al., 2000), suggesting a direct correlation between NDST expression and the level of HS sulphation. It is possible that these changes are

not limited to HS; indeed, a recent study has shown that over-sulphation of HS in cells which express high levels of NDST-1 is associated with decreased sulphation of chondroitin sulphate (Bengtsson, 2003). A previous study has also shown that treatment of endothelial cells with TNF-α or IFN-γ can increase the incorporation of sulphate into HS within a similar timescale to that observed in the current work, but the mechanism for this was not defined (Klein, 1992). Further work will be required to characterise the HS species produced by cytokine-stimulated HMEC-1, but it is now apparent that the change in sulphation correlates with an increased ability of the cells to bind the chemokine RANTES. This is consistent with a demonstration that the extent of HS sulphation varies between endothelial cells from different sites, with the highly sulphated HS expressed by bone marrow endothelium having a high affinity for the chemokine SDF-1 (Netelenbos, 2001).

The binding of RANTES to HMEC-1 is restricted to cell surface GAGs as these cells do not express specific receptors for this chemokine. Indeed, the only specific chemokine receptor that has been demonstrated on endothelial cells is CXCR4 (Volin et al., 1998), which binds the chemokine SDF-1; the RANTES receptors CCR2 and CCR5 are restricted to leukocytes (Mack et al., 1999; Qin et al., 1998; Sorensen et al., 1999), and DARC was expressed at a constant low level. As RANTES is known to bind to highly sulphated domains on HS (Mbemba et al., 2001), it is most likely that the increased binding of this chemokine observed after endothelial cell activation is a specific consequence of a chlorate-inhibitable, heparitinase-sensitive, NDST-mediated increase in cell surface expression of sulphated HS. This observation has implications for previous studies that have attempted to measure cell surface chemokine binding. Variable results from these studies (Ali et al., 2000; Appay et al., 1999; Mbemba et al., 2001) could simply reflect natural changes in the extent of sulphation of the HS expressed by particular cell types.

In separate studies our group has shown that the sequestration of chemokines to cell surface GAGs can increase the biological activity of these factors and is an essential prerequisite for chemokine-mediated migration of leukocytes across cell monolayers (Ali et al., 2002; Ali et al., 2000). The current study demonstrated that treatment of the HMEC-1 model endothelium with TNF-α and IFN-γ does not increase transendothelial migration of THP-1 monocytes, but cytokine-activation does synergise with subendothelial RANTES to induce a greatly enhanced chemotactic response. It is likely that the activation of endothelial cells by TNF-α and IFN-γ is necessary for efficient chemokine sequestration and presentation by the endothelium, leading to the induction of leukocyte migration from the apical to the basal surface of the endothelium. Indeed, the reduced potential of undersulphated HS to bind chemokines to the surface of resting endothelium could prevent non-specific inflammation from occurring as a consequence of inappropriate sequestration of circulating chemokines by normal vascular endothelial cells.

The authors would like to thank Drs Vyki Conlin and Trevor Booth for help and advice during the confocal microscopic study. This work was supported by grants from the Wellcome Trust (grant 054268/98) and the British Heart Foundation (project grant PG/99141).

References

Adams, D. H. and Lloyd, A. R. (1997). Chemokines: leucocyte recruitment and activation cytokines. *Lancet* **349**, 490-495.

Ades, E. W., Candal, F. J., Swerlick, R. A., George, V. G., Summers, S., Bosse, D. C. and Lawley, T. J. (1992). HMEC-1 – Establishment of an Immortalized Human Microvascular Endothelial-Cell Line. *J. Invest. Dermatol.* **99**, 683-690.

Aikawa, J., Grobe, K., Tsujimoto, M. and Esko, J. D. (2001). Multiple isozymes of heparan sulfate/heparin GlcNAc N-deacetylase/GlcN N-sulfotransferase. Structure and activity of the fourth member, NDST4. *J. Biol. Chem.* **276**, 5876-5882.

Ali, S., Fritchley, S., Chaffey, B. T. and Kirby, J. A. (2002). Contribution of the putative heparan-sulphate binding motif BBXB of RANTES to transendothelial migration. *Glycobiology* **12**, 535-543.

Ali, S., Palmer, A. C., Banerjee, B., Fritchley, S. J. and Kirby, J. A. (2000). Examination of the function of RANTES, MIP-1alpha, and MIP-1beta following interaction with heparin-like glycosaminoglycans. *J. Biol. Chem.* **275**, 11721-11727.

Appay, V., Brown, A., Cribbes, S., Randle, E. and Czaplewski, L. G. (1999). Aggregation of RANTES is responsible for its inflammatory properties. Characterization of nonaggregating, noninflammatory RANTES mutants. *J. Biol. Chem.* **274**, 27505-27512.

Appay, V. and Rowland-Jones, S. L. (2001). RANTES: a versatile and controversial chemokine. *Trends Immunol.* **22**, 83-87.

Bengtsson, J., Eriksson, I. and Kjellan, L. (2003). Distinct effects on heparan sulphate structure by different active site mutations in NDST-1. *Biochemistry* **42**, 2110-2115.

Bosse, D., George, V., Candal, F. J., Lawley, T. J. and Ades, E. W. (1993). Antigen presentation by a continuous human microvascular endothelial-cell line, HMEC-1, to human T-cells. *Pathobiology* **61**, 236-238.

Butterfield, J. H., Weiler, D., Dewald, G. and Gleich, G. J. (1988). Establishment of an immature mast cell line from a patient with mast cell leukemia. *Leuk. Res.* **12**, 345-355.

Cheung, W. F., Eriksson, I., Kusche-Gullberg, M., Lindhal, U. and Kjellen, L. (1996). Expression of the mouse mastocytoma glucosaminyl N-deacetylase/N-sulfotransferase in human kidney 293 cells results in increased N-sulfation of heparan sulfate. *Biochemistry* **35**, 5250-5256.

Cockwell, P., Adams, D. H. and Savage, C. O. (1996). Glycosaminoglycans contribute to multiple functions of vascular endothelial cells. *Clin. Exp. Immunol.* **104**, 1-3.

David, G., Bai, X. M., Van der Schueren, B., Cassiman, J. J. and Van den Berghe, H. (1992). Developmental changes in heparan sulfate expression: in situ detection with mAbs. *J. Cell Biol.* **119**, 961-975.

Dixon, J., Loftus, S. K., Gladwin, A. J., Scambler, P. J., Wasmuth, J. J. and Dixon, M. J. (1995). Cloning of the human heparan sulfate-N-deacetylase/N-sulfotransferase gene from the Treacher Collins syndrome candidate region at 5q32-q33.1. *Genomics* **26**, 239-244.

Esko, J. (2002). *Preparation and Analysis of Glycoconjugates.* New York: John Wiley and Sons.

Gallagher, J. T. (1997). Structure-activity relationship of heparan sulphate. *Biochem. Soc. Trans.* **25**, 1206-1209.

Goebeler, M., Yoshimura, T., Toksoy, A., Ritter, U., Brocker, E. B. and Gillitzer, R. (1997). The chemokine repertoire of human dermal microvascular endothelial cells and its regulation by inflammatory cytokines. *J. Invest. Dermatol.* **108**, 445-451.

Grobe, K. and Esko, J. D. (2002). Regulated translation of heparan sulfate N-acetylglucosamine N-deacetylase/N-sulfotransferase isozymes by structured 5′-untranslated regions and internal ribosome entry sites. *J. Biol. Chem.* **277**, 30699-30706.

Habuchi, H., Tanaka, M., Habuchi, O., Yoshida, K., Suzuki, H., Ban, K. and Kimata, K. (2000). The occurrence of three isoforms of heparan sulfate 6-O-sulfotransferase having different specificities for hexuronic acid adjacent to the targeted N-sulfoglucosamine. *J. Biol. Chem.* **275**, 2859-2868.

Hileman, R. E., Fromm, J. R., Weiler, J. M. and Linhardt, R. J. (1998). Glycosaminoglycan-protein interactions: definition of consensus sites in glycosaminoglycan binding proteins. *BioEssays* **20**, 156-167.

Humphries, D. E., Lanciotti, J. and Karlinsky, J. B. (1998). cDNA cloning, genomic organization and chromosomal localization of human heparan glucosaminyl N-deacetylase/N-sulphotransferase-2. *Biochem. J.* **332**, 303-307.

Klein, N. J., Shennan, G. I., Heyderman, R. S. and Levin, M. (1992). Alteration in glycosaminoglycan metabolism and surface charge on human umbilical vein endothelial cells induced by cytokines, endotoxin and neutrophils. *J. Cell Sci.* **102**, 821-832.

Kusche-Gullberg, M., Eriksson, I., Pikas, D. S. and Kjellen, L. (1998). Identification and expression in mouse of two heparan sulfate glucosaminyl N-deacetylase/N-sulfotransferase genes. *J. Biol. Chem.* **273**, 11902-11907.

Kuschert, G. S., Coulin, F., Power, C. A., Proudfoot, A. E., Hubbard, R. E., Hoogewerf, A. J. and Wells, T. N. (1999). Glycosaminoglycans interact selectively with chemokines and modulate receptor binding and cellular responses. *Biochemistry* **38**, 12959-12968.

Li, J., Hagner-McWhirter, A., Kjellen, L., Palgi, J., Jalkanen, M. and Lindahl, U. (1997). Biosynthesis of heparin/heparan sulfate. cDNA cloning and expression of D-glucuronyl C5-epimerase from bovine lung. *J. Biol. Chem.* **272**, 28158-28163.

Lortat-Jacob, H., Turnbull, J. E. and Grimaud, J. A. (1995). Molecular organization of the interferon gamma-binding domain in heparan sulphate. *Biochem. J.* **310**, 497-505.

Mack, M., Bruhl, H., Gruber, R., Jaeger, C., Cihak, J., Eiter, V., Plachy, J., Stangassinger, M., Uhlig, K., Schattenkirchner, M. et al. (1999). Predominance of mononuclear cells expressing the chemokine receptor CCR5 in synovial effusions of patients with different forms of arthritis. *Arthritis Rheum* **42**, 981-988.

Mantovani, A., Sozzani, S. and Introna, M. (1997). Endothelial activation by cytokines. *Ann. N.Y. Acad. Sci.* **832**, 93-116.

Mbemba, E., Slimani, H., Atemezem, A., Saffar, L. and Gattegno, L. (2001). Glycans are involved in RANTES binding to CCR5 positive as well as to CCR5 negative cells. *Biochim. Biophys. Acta.* **1510**, 354-366.

Morita, H., Shinzato, T., David, G., Mizutani, A., Habuchi, H., Fujita, Y., Ito, M., Asai, J., Maeda, K. and Kimata, K. (1994). Basic fibroblast growth factor-binding domain of heparan sulfate in the human glomerulosclerosis and renal tubulointerstitial fibrosis. *Lab. Invest.* **71**, 528-535.

Neish, A. S., Khachigian, L. M., Park, A., Baichwal, V. R. and Collins, T. (1995). Sp1 is a component of the cytokine-inducible enhancer in the promoter of vascular cell adhesion molecule-1. *J. Biol. Chem.* **270**, 28903-28909.

Netelenbos, T., Drager, A. M., van het Hof, B., Kessler, F. L., Delouis, C., Huijgens, P. C., van den Born, J. and van Dijk, W. (2001). Differential sulphation patterns of heparan sulphate derived from human bone marrow and umbilical vein endothelial cells. *Exp. Hematol.* **29**, 884-893.

Olofsson, A. M., Vestberg, M., Herwald, H., Rygaard, J., David, G., Arfors, K. E., Linde, V., Flodgaard, H., Dedio, J., Muller-Esterl, W. et al. (1999). Heparin-binding protein targeted to mitochondrial compartments protects endothelial cells from apoptosis. *J. Clin. Invest.* **104**, 885-894.

Orellana, A., Hirschberg, C. B., Wei, Z., Swiedler, S. J. and Ishihara, M. (1994). Molecular cloning and expression of a glycosaminoglycan N-acetylglucosaminyl N-deacetylase/N-sulfotransferase from a heparin-producing cell line. *J. Biol. Chem.* **269**, 2270-2276.

Patel, D. D., Koopmann, W., Imai, T., Whichard, L. P., Yoshie, O. and Krangel, M. S. (2001). Chemokines have diverse abilities to form solid phase gradients. *Clin. Immunol.* **99**, 43-52.

Perrimon, N. and Bernfield, M. (2000). Specificities of heparan sulphate proteoglycans in developmental processes. *Nature* **404**, 725-728.

Pikas, D. S., Eriksson, I. and Kjellen, L. (2000). Overexpression of different isoforms of glucosaminyl N-deacetylase/N-sulfotransferase results in distinct heparan sulfate N-sulfation patterns. *Biochemistry* **39**, 4552-4558.

Praillet, C., Lortat-Jacob, H., Baltzer, F. and Grimaud, J. A. (1996a). Distribution of hepatic glycosaminoglycans during acute schistosomiasis: modulation by IFN gamma treatment. *Cell. Mol. Biol.* **42**, 169-177.

Praillet, C., Lortat-Jacob, H. and Grimaud, J. A. (1996b). Interferon gamma differentially affects the synthesis of chondroitin/dermatan sulphate and heparan sulphate by human skin fibroblasts. *Biochem. J.* **318**, 863-870.

Praillet, C., Lortat-Jacob, H. and Grimaud, J. A. (1996c). Interferon-gamma inhibits 35S incorporation in heparan sulfate synthesized by human skin fibroblasts. *FEBS Lett.* **387**, 109-112.

Proudfoot, A. E., Fritchley, S., Borlat, F., Shaw, J. P., Vilbois, F., Zwahlen, C., Trkola, A., Marchant, D., Clapham, P. R. and Wells, T. N. (2001). The BBXB motif of RANTES is the principal site for heparin binding and controls receptor selectivity. *J. Biol. Chem.* **276**, 10620-10626.

Pye, D. A., Vives, R. R., Turnbull, J. E., Hyde, P. and Gallagher, J. T. (1998). Heparan sulfate oligosaccharides require 6-O-sulfation for promotion of basic fibroblast growth factor mitogenic activity. *J. Biol. Chem.* **273**, 22936-22942.

Qin, S., Rottman, J. B., Myers, P., Kassam, N., Weinblatt, M., Loetscher, M., Koch, A. E., Moser, B. and Mackay, C. R. (1998). The chemokine receptors CXCR3 and CCR5 mark subsets of T cells associated with certain inflammatory reactions. *J. Clin. Invest.* **101**, 746-754.

Rix, D. A., Douglas, M. S., Talbot, D., Dark, J. H. and Kirby, J. A. (1996). Role of glycosaminoglycans (GAGs) in regulation of the immunogenicity of human vascular endothelial cells. *Clin. Exp. Immunol.* **104**, 60-65.

Robinson, M. J., Tessier, P., Poulsom, R. and Hogg, N. (2002). The S100 family heterodimer, MRP-8/14, binds with high affinity to heparin and heparan sulfate glycosaminoglycans on endothelial cells. *J. Biol. Chem.* **277**, 3658-3665.

Rot, A., Hub, E., Middleton, J., Pons, F., Rabeck, C., Thierer, K., Wintle, J., Wolff, B., Zsak, M. and Dukor, P. (1996). Some aspects of IL-8 pathophysiology. III: Chemokine interaction with endothelial cells. *J. Leuk. Biol.* **59**, 39-44.

Safaiyan, F., Kolset, S. O., Prydz, K., Gottfridsson, E., Lindahl, U. and Salmivirta, M. (1999). Selective effects of sodium chlorate treatment on the sulfation of heparan sulfate. *J. Biol. Chem.* **274**, 36267-36273.

Shworak, N. W., Liu, J., Petros, L. M., Zhang, L., Kobayashi, M., Copeland, N. G., Jenkins, N. A. and Rosenberg, R. D. (1999). Multiple isoforms of heparan sulfate D-glucosaminyl 3-O-sulfotransferase. Isolation, characterization, and expression of human cdnas and identification of distinct genomic loci. *J. Biol. Chem.* **274**, 5170-5184.

Sorensen, T. L., Tani, M., Jensen, J., Pierce, V., Lucchinetti, C., Folcik, V. A., Qin, S., Rottman, J., Sellebjerg, F., Strieter, R. M. et al. (1999). Expression of specific chemokines and chemokine receptors in the central nervous system of multiple sclerosis patients. *J. Clin. Invest.* **103**, 807-815.

Tanaka, Y., Kimata, K., Wake, A., Mine, S., Morimoto, I., Yamakawa, N., Habuchi, H., Ashikari, S., Yamamoto, H., Sakurai, K. et al. (1996). Heparan sulfate proteoglycan on leukemic cells is primarily involved in integrin triggering and its mediated adhesion to endothelial cells. *J. Exp. Med.* **184**, 1987-1997.

Toma, L., Berninsone, P. and Hirschberg, C. B. (1998). The putative heparin-specific N-acetylglucosaminyl N-Deacetylase/N-sulfotransferase also occurs in non-heparin-producing cells. *J. Biol. Chem.* **273**, 22458-22465.

Unger, E., Pettersson, I., Eriksson, U. J., Lindahl, U. and Kjellen, L. (1991). Decreased activity of the heparan sulfate-modifying enzyme glucosaminyl N-deacetylase in hepatocytes from streptozotocin-diabetic rats. *J. Biol. Chem.* **266**, 8671-8674.

Volin, M. V., Joseph, L., Shockley, M. S. and Davies, P. F. (1998). Chemokine receptor CXCR4 expression in endothelium. *Biochem. Biophys. Res. Commun.* **242**, 46-53.

Voraberger, G., Schafer, R. and Stratowa, C. (1991). Cloning of the human gene for intercellular adhesion molecule 1 and analysis of its 5′-regulatory region. Induction by cytokines and phorbol ester. *J. Immunol.* **147**, 2777-2786.

Witt, D. P. and Lander, A. D. (1994). Differential binding of chemokines to glycosaminoglycan subpopulations. *Curr. Biol.* **4**, 394-400.